

Domain wall motion in ferromagnetic nanotubes: Analytic results

Arseni Goussev^{1,2}, JM Robbins³, Valeriy Slastikov³

¹Department of Mathematics and Information Sciences,

Northumbria University, Newcastle Upon Tyne, NE1 8ST, United Kingdom

²Max Planck Institute for the Physics of Complex Systems,

Nöthnitzer Straße 38, D-01187 Dresden, Germany

³School of Mathematics, University of Bristol, University Walk, Bristol, BS8 1TW, United Kingdom

(Dated: June 29, 2021)

Dynamics of magnetization domain walls (DWs) in thin ferromagnetic nanotubes subject to longitudinal external fields is addressed analytically in the regimes of strong and weak penalization. Explicit functional forms of the DW profiles and formulas for the DW propagation velocity are derived in both regimes. In particular, the DW speed is shown to depend nonlinearly on the nanotube radius.

PACS numbers: 75.75.-c, 75.78.Fg

The problem of controlled manipulation of magnetization domains in quasi-one-dimensional ferromagnetic nanostructures is of paramount technological importance in designing new generation memory devices [1–3] and of fundamental interest in the vibrant areas of micromagnetics and spintronics. To date, substantial theoretical progress has been achieved in understanding the dynamics of domain walls (DWs) in nanowires under the influence of applied magnetic fields [4–15] and spin-polarized electric currents [15–23]. Nevertheless, the search for schemes and regimes allowing fast and energy efficient DW propagation actively continues.

Recently, ferromagnetic nanotubes have been proposed as a guide of DWs driven by an external magnetic field [24]. The central advantage of this approach is the absence of the so-called Walker breakdown that is unavoidable at sufficiently strong applied fields for wire and strip geometries [4]. The absence of the Walker breakdown is a topological effect which leads to a significant increase of the DW stability and propagation speed [24, 25].

In this paper, we analytically address the DW dynamics in thin ferromagnetic nanotubes under the action of an external magnetic field and derive an explicit formula for the DW propagation speed in the regimes of strong and weak penalization. Our formula reveals a nonlinear dependence of the propagation speed on the nanotube radius, and may be used as a guide in devising new experiments.

We consider an infinitely long ferromagnetic nanotube with an outer radius R and an inner radius $(R - w)$ (see Fig. 1). The magnetization distribution at a spatial point \mathbf{x} and time t is described by $\mathbf{M}(\mathbf{x}, t) = M_s \mathbf{m}(\mathbf{x}, t)$, where $|\mathbf{m}(\mathbf{x}, t)| = 1$ if $\mathbf{x} \in \Omega$ (the point belongs to the nanotube region) and $|\mathbf{m}(\mathbf{x}, t)| = 0$ if $\mathbf{x} \notin \Omega$ (the point lies outside the nanotube region). Here, M_s stands for the saturation magnetization. The full micromagnetic energy of

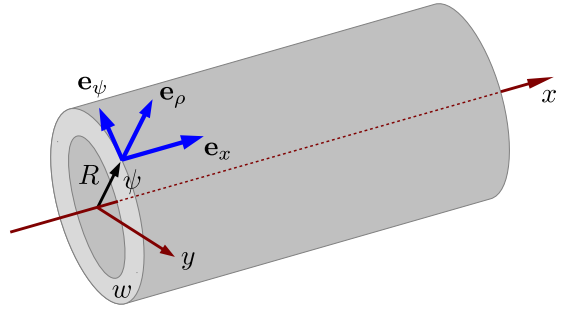


FIG. 1: (Color online) A sketch of a nanotube with an outer radius R and an inner radius $R - w$. A point on the outer surface of the nanotube is parametrized by the coordinate x along its symmetry axis and the polar angle ψ . The unit vectors \mathbf{e}_x (parallel to the symmetry axis), \mathbf{e}_ψ (tangential to the surface), and \mathbf{e}_ρ (normal to the surface) form a right-handed triplet.

the nanotube is given by [26]

$$E(\mathbf{m}) = A \int_{\Omega} |\nabla \mathbf{m}|^2 d\mathbf{x} + K \int_{\Omega} [1 - (\mathbf{m} \cdot \mathbf{e}_x)^2] d\mathbf{x} + \frac{\mu_0 M_s^2}{2} \int_{\mathbb{R}^3} |\nabla u|^2 d\mathbf{x}, \quad (1)$$

where the magnetostatic potential $u(\mathbf{x}, t)$ satisfies

$$\nabla \cdot (\nabla u + \mathbf{m}) = 0 \quad \text{for } \mathbf{x} \in \mathbb{R}^3. \quad (2)$$

Here, A denotes the exchange constant, K is the easy axis anisotropy constant, $\mu_0 = 4\pi \times 10^{-7}$ Wb/(A·m) is the magnetic permeability of vacuum, and \mathbf{e}_x is a unit vector pointing along the symmetry axis (x -axis) of the nanotube (see Eq. 1).

Within a continuum description, the time evolution of the magnetization distribution is governed by the Landau-Lifshitz (LL) equation [27, 28]

$$\frac{\partial \mathbf{m}}{\partial t} = \gamma \mathbf{m} \times \mathbf{H} - \alpha \mathbf{m} \times (\mathbf{m} \times \mathbf{H}). \quad (3)$$

Here, γ denotes the gyromagnetic ratio, α is a phenomenological damping parameter, and \mathbf{H} is an effective magnetic field, given by

$$\mathbf{H}(\mathbf{m}) = -\frac{1}{\mu_0 M_s} \frac{\delta E}{\delta \mathbf{m}} + \mathbf{H}_a, \quad (4)$$

where \mathbf{H}_a stands for the applied (external) magnetic field. Being interested in the dynamics of a magnetization domain wall (DW), we focus on solutions of Eq. (3) subject to the boundary conditions $\mathbf{m}(\mathbf{x}, t) \rightarrow \pm \mathbf{e}_x$ for $x \rightarrow \pm\infty$ (and $\mathbf{x} \in \Omega$).

We now address the case of a thin nanotube, such that $w \ll R$. In this limit, the volume integrals in Eq. (1) can be approximately reduced to integrals over the surface of a cylinder, and the stray-field energy can be approximated by an additional effective local anisotropy that penalises the magnetisation component in the radial direction (see [29, 30] for mathematical details of this procedure). Thus, rescaling the spatial variables, $\mathbf{x} = R\xi$; the micromagnetic energy, $E = 2Aw\mathcal{E}$; and the effective and applied fields, $\mathbf{H} = [2A/(\mu_0 M_s R^2)]\mathbf{H}$ and $\mathbf{H}_a = [2A/(\mu_0 M_s R^2)]\mathbf{H}_a$, we approximate Eqs. (1–4) by

$$\begin{aligned} \mathcal{E}(\mathbf{m}) = & \frac{1}{2} \int_S |\nabla_S \mathbf{m}|^2 d\sigma + \frac{\kappa}{2} \int_S [1 - (\mathbf{m} \cdot \mathbf{e}_x)^2] d\sigma \\ & + \frac{\lambda}{2} \int_S (\mathbf{m} \cdot \mathbf{e}_\rho)^2 d\sigma \end{aligned} \quad (5)$$

and

$$\mathcal{H}(\mathbf{m}) = \nabla_S^2 \mathbf{m} + \kappa(\mathbf{m} \cdot \mathbf{e}_x)\mathbf{e}_x - \lambda(\mathbf{m} \cdot \mathbf{e}_\rho)\mathbf{e}_\rho + \mathbf{H}_a, \quad (6)$$

where $\kappa = KR^2/A$ and $\lambda = \mu_0 M_s^2 R^2/(2A)$. The integrals in Eq. (5) run over the surface of an infinitely long cylinder of unit radius, and $\nabla_S = \mathbf{e}_x \frac{\partial}{\partial \xi} + \mathbf{e}_\psi \frac{\partial}{\partial \psi}$ represents the surface gradient (and, accordingly, $\nabla_S^2 = \frac{\partial^2}{\partial \xi^2} + \frac{\partial^2}{\partial \psi^2}$ the surface Laplacian). Consequently, rescaling the time variable as $t = [\mu_0 M_s R^2/(2\gamma A)]\tau$, we rewrite the LL equation (3) in the dimensionless form,

$$\frac{\partial \mathbf{m}}{\partial \tau} = \mathbf{m} \times \mathcal{H} - \frac{\alpha}{\gamma} \mathbf{m} \times (\mathbf{m} \times \mathcal{H}). \quad (7)$$

Equations (5–7), along with the boundary condition $\mathbf{m}(\xi, \tau) \rightarrow \pm \mathbf{e}_x$ as $\xi \rightarrow \pm\infty$ specify the magnetization dynamics problem addressed in this paper. Below, we provide exact, traveling wave solutions to this problem in the two limiting cases of $\lambda \gg 1$ and $\lambda \ll 1$.

Strong penalization case, $\lambda \gg 1$. – In ferromagnetic nanotubes with very large λ , the penalization term in the micromagnetic energy, Eq. (5), essentially forces the magnetization distribution \mathbf{m} to lie nearly tangent to the cylinder (see Fig. 2). More specifically, it can be shown that $\mathbf{m} = \mathbf{m}_t + \lambda^{-1} \mathbf{m}_n$, where $\mathbf{m}_t = (\mathbf{m} \cdot \mathbf{e}_x)\mathbf{e}_x + (\mathbf{m} \cdot \mathbf{e}_\psi)\mathbf{e}_\psi$ is tangent to the cylinder and $\mathbf{m}_n = (\mathbf{m} \cdot \mathbf{e}_\rho)\mathbf{e}_\rho$ (with $|\mathbf{m}_n| \sim \mathcal{O}(1)$) is normal to the cylinder surface.

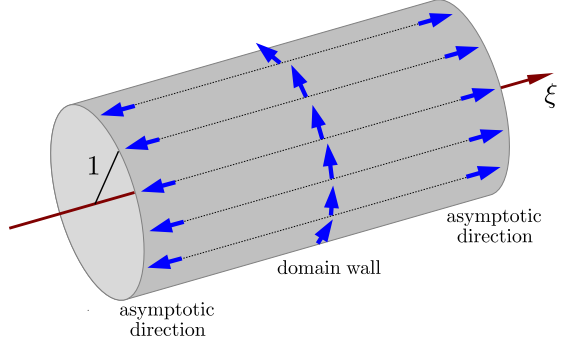


FIG. 2: (Color online) A sketch of a magnetization DW for the case of $\lambda \gg 1$.

Resolving the effective field into its tangential and normal components $\mathcal{H}_t = (\mathcal{H} \cdot \mathbf{e}_x)\mathbf{e}_x + (\mathcal{H} \cdot \mathbf{e}_\psi)\mathbf{e}_\psi$ and $\mathcal{H}_n = (\mathcal{H} \cdot \mathbf{e}_\rho)\mathbf{e}_\rho$ (both $|\mathcal{H}_t|$ and $|\mathcal{H}_n|$ being of order 1), we rewrite Eq. (7) as $\frac{d}{d\tau} \mathbf{m}_t = \mathbf{m}_t \times (\mathcal{H}_t + \mathcal{H}_n) - \frac{\alpha}{\gamma} \mathbf{m}_t \times [\mathbf{m}_t \times (\mathcal{H}_t + \mathcal{H}_n)] + \mathcal{O}(\lambda^{-1})$. Then, resolving this equation into its tangential and normal components and keeping terms of the leading order in λ^{-1} , we obtain

$$\frac{d}{d\tau} \mathbf{m}_t = \mathbf{m}_t \times \mathcal{H}_n - \frac{\alpha}{\gamma} \mathbf{m}_t \times (\mathbf{m}_t \times \mathcal{H}_t), \quad (8)$$

$$0 = \mathbf{m}_t \times \mathcal{H}_t - \frac{\alpha}{\gamma} \mathbf{m}_t \times (\mathbf{m}_t \times \mathcal{H}_n). \quad (9)$$

Taking the cross product of both sides of Eq. (9) with \mathbf{m}_t , and using $|\mathbf{m}_t|^2 = 1 + \mathcal{O}(\lambda^{-2})$ we obtain, to the leading order in λ^{-1} ,

$$\mathbf{m}_t \times \mathcal{H}_n = -\frac{\gamma}{\alpha} \mathbf{m}_t \times (\mathbf{m}_t \times \mathcal{H}_t). \quad (10)$$

Finally, substituting Eq. (10) into Eq. (8), we conclude that, in the limit $\lambda \rightarrow \infty$ (or, more generally, in the leading order in λ^{-1}) the time evolution of $\mathbf{m}(\xi, \psi, \tau)$ is governed by the modified LL equation,

$$\frac{\partial \mathbf{m}}{\partial \tau} = -\left(\frac{\alpha}{\gamma} + \frac{\gamma}{\alpha}\right) \mathbf{m} \times (\mathbf{m} \times \mathcal{H}_t), \quad (11)$$

where the magnetization distribution is restricted to be tangent to the surface of the cylinder,

$$\mathbf{m} = \mathbf{e}_x \cos \theta + \mathbf{e}_\psi \sin \theta. \quad (12)$$

In general, $\theta = \theta(\xi, \psi, \tau)$. A similar result has been obtained for the effective dynamics in thin ferromagnetic films [31].

We now assume that the applied magnetic field is directed along the nanotube axis, $\mathcal{H}_a = \mathcal{H}_a \mathbf{e}_x$. Substituting Eq. (12) into Eq. (6), taking into account the fact that $\frac{\partial}{\partial \psi} \mathbf{e}_\psi = -\mathbf{e}_\rho$ and $\frac{\partial}{\partial \psi} \mathbf{e}_\rho = \mathbf{e}_\psi$, and discarding the component of \mathcal{H} along \mathbf{e}_ρ , we obtain the tangential component of the effective field,

$$\begin{aligned} \mathcal{H}_t = & (-\sin \theta \nabla_S^2 \theta - \cos \theta |\nabla_S \theta|^2 + \kappa \cos \theta + \mathcal{H}_a) \mathbf{e}_x \\ & + (\cos \theta \nabla_S^2 \theta - \sin \theta |\nabla_S \theta|^2 - \sin \theta) \mathbf{e}_\psi. \end{aligned} \quad (13)$$

Consequently,

$$\mathbf{m} \times (\mathbf{m} \times \mathcal{H}_t) = (\nabla_S^2 \theta - (1 + \kappa) \sin \theta \cos \theta - \mathcal{H}_a \sin \theta) (\mathbf{e}_x \sin \theta - \mathbf{e}_\psi \cos \theta). \quad (14)$$

Thus, using the identity $\frac{\partial}{\partial \tau} \mathbf{m} = -(\mathbf{e}_x \sin \theta - \mathbf{e}_\psi \cos \theta) \frac{\partial}{\partial \tau} \theta$ and Eq. (14) in the left- and right-hand side of Eq. (11) respectively, we obtain

$$\frac{\partial \theta}{\partial \tau} = \left(\frac{\alpha}{\gamma} + \frac{\gamma}{\alpha} \right) (\nabla_S^2 \theta - (1 + \kappa) \sin \theta \cos \theta - \mathcal{H}_a \sin \theta). \quad (15)$$

Equation (15) governs the dynamics of the magnetization distribution, given by Eq. (12), subject to the boundary conditions $\lim_{\xi \rightarrow -\infty} \theta(\xi, \psi, \tau) = \pi$ and $\lim_{\xi \rightarrow +\infty} \theta(\xi, \psi, \tau) = 0$. It can be straightforwardly verified that this problem admits a family of exact traveling wave solutions

$$\theta(\xi, \psi, \tau) = \Theta_1(\xi - \xi_0(\tau)), \quad (16)$$

where the function

$$\Theta_1(\xi) = 2 \tan^{-1} \exp(-\xi \sqrt{1 + \kappa}) \quad (17)$$

(or, equivalently, $\frac{d}{d\xi} \Theta_1 = -\sqrt{1 + \kappa} \sin \Theta_1$) determines the spatial profile of the traveling wave, and

$$\frac{d\xi_0}{d\tau} = -\left(\frac{\alpha}{\gamma} + \frac{\gamma}{\alpha}\right) \frac{\mathcal{H}_a}{\sqrt{1 + \kappa}} \quad (18)$$

gives the propagation velocity. In the original physical coordinates, the propagation velocity reads

$$\frac{dx_0}{dt} = -\left(\frac{\alpha}{\gamma} + \frac{\gamma}{\alpha}\right) \frac{\gamma R \mathcal{H}_a}{\sqrt{1 + KR^2/A}}. \quad (19)$$

Equation (19) gives explicitly the nonlinear dependence of the DW propagation speed on the nanotube radius. Thus, in the anisotropic case ($K > 0$), our formula shows that $|\frac{d}{dt} x_0| \propto R \mathcal{H}_a$ for $R \ll \sqrt{A/K}$, and $|\frac{d}{dt} x_0| \propto H_a$ for $R \gg \sqrt{A/K}$. In the isotropic case ($K = 0$), however, $|\frac{d}{dt} x_0| \propto R \mathcal{H}_a$ at any nanotube radius.

Weak penalization case, $\lambda \ll 1$. – We now focus on the case of a ferromagnetic nanotube for which the penalization parameter λ is negligibly small. In this case the magnetization distribution \mathbf{m} is no longer restricted to lie tangent to the cylinder and explores the full unit sphere. Its time evolution is governed by the LL equation (7) with the effective field approximated by (cf. Eq. (6))

$$\mathcal{H} = \nabla_S^2 \mathbf{m} + (\kappa \mathbf{m} \cdot \mathbf{e}_x + \mathcal{H}_a) \mathbf{e}_x. \quad (20)$$

Substituting the Cartesian representation of the magnetization distribution, $\mathbf{m} = (\cos \theta, \sin \theta \cos \phi, \sin \theta \sin \phi)$, into Eqs. (7) and (20), we

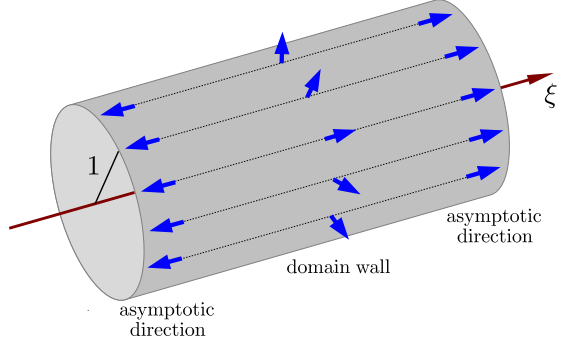


FIG. 3: (Color online) A sketch of the magnetization DW for the case of $\lambda \ll 1$. The DW has the helicity index $n = 1$.

obtain a system of two coupled nonlinear PDEs for the unknown functions $\theta = \theta(\xi, \psi, \tau)$ and $\phi = \phi(\xi, \psi, \tau)$:

$$\frac{\partial \theta}{\partial \tau} + \frac{\gamma}{\alpha} \frac{\partial \phi}{\partial \tau} \sin \theta = \left(\frac{\alpha}{\gamma} + \frac{\gamma}{\alpha} \right) \mathcal{F}_1, \quad (21)$$

$$-\frac{\gamma}{\alpha} \frac{\partial \theta}{\partial \tau} + \frac{\partial \phi}{\partial \tau} \sin \theta = \left(\frac{\alpha}{\gamma} + \frac{\gamma}{\alpha} \right) \mathcal{F}_2, \quad (22)$$

where

$$\mathcal{F}_1 = \frac{\partial^2 \theta}{\partial \xi^2} + \frac{\partial^2 \theta}{\partial \psi^2} - \left[\kappa + \left(\frac{\partial \phi}{\partial \xi} \right)^2 + \left(\frac{\partial \phi}{\partial \psi} \right)^2 \right] \sin \theta \cos \theta - \mathcal{H}_a \sin \theta, \quad (23)$$

$$\mathcal{F}_2 = 2 \left[\frac{\partial \theta}{\partial \xi} \frac{\partial \phi}{\partial \xi} + \frac{\partial \theta}{\partial \psi} \frac{\partial \phi}{\partial \psi} \right] \cos \theta + \left[\frac{\partial^2 \phi}{\partial \xi^2} + \frac{\partial^2 \phi}{\partial \psi^2} \right] \sin \theta. \quad (24)$$

As before, this system is to be solved subject to the boundary conditions $\lim_{\xi \rightarrow -\infty} \theta(\xi, \psi, \tau) = \pi$ and $\lim_{\xi \rightarrow +\infty} \theta(\xi, \psi, \tau) = 0$.

As can be readily verified by a direct substitution, this problem admits a two-parameter family of exact traveling wave solutions

$$\theta(\xi, \psi, \tau) = \Theta_n(\xi - \xi_0(\tau)), \quad (25)$$

$$\phi(\xi, \psi, \tau) = n\psi + \Phi(\tau), \quad (26)$$

with $n \in \mathbb{Z}$. Here, the longitudinal profile of the DW is given by

$$\Theta_n(\xi) = 2 \tan^{-1} \exp(-\xi \sqrt{n^2 + \kappa}) \quad (27)$$

(or, equivalently, $\frac{d}{d\xi} \Theta_n = -\sqrt{n^2 + \kappa} \sin \Theta_n$), the precession velocity by

$$\frac{d\Phi}{d\tau} = -\mathcal{H}_a, \quad (28)$$

and the propagation velocity by

$$\frac{d\xi_0}{d\tau} = -\frac{\alpha}{\gamma} \frac{\mathcal{H}_a}{\sqrt{n^2 + \kappa}}. \quad (29)$$

In the original physical coordinates, the propagation velocity reads

$$\frac{dx_0}{dt} = -\frac{\alpha RH_a}{\sqrt{n^2 + KR^2/A}}. \quad (30)$$

In Eqs. (25–30), the index n measures the DW helicity. That is, n counts the number of times that the magnetization vector turns about \mathbf{e}_x as the circumference of the cylinder is traversed. (A sketch of a DW with $n = 1$ is shown in Fig. 3.) It is interesting to note that DWs with lower helicity propagate faster, with the maximal propagation speed, $|\frac{dx_0}{dt}| = (\alpha/\gamma)|H_a|/\sqrt{\kappa}$, achieved for $n = 0$.

As in the strong penalization case, Eq. (30) gives the full nonlinear dependence of the DW propagation speed on the nanotube radius. In the anisotropic case ($K > 0$), we see that $|\frac{dx_0}{dt}| \propto RH_a$ for $R \ll n\sqrt{A/K}$, while $|\frac{dx_0}{dt}| \propto H_a$ for $R \gg n\sqrt{A/K}$. In the isotropic case ($K = 0$), we again recover the scaling $|\frac{dx_0}{dt}| \propto RH_a$.

In conclusion, we have conducted an analytic study of the DW dynamics in thin ferromagnetic nanotubes subject to external longitudinal magnetic fields. We have found explicit functional forms of the DW profiles and derived explicit formulas for the DW velocity in the regimes of strong and weak penalization, Eqs. (19) and (30) respectively. In the strong penalization case, the magnetization field lies nearly tangent to the nanotube, while for weak penalizations, the magnetization vector may wrap around the nanotube with any integer helicity index. The DW propagation speed increases with the nanotube radius in a nonlinear way, and, in the weak penalization case, decreases with increasing helicity. Since for a typical ferromagnetic material $\alpha/\gamma \ll 1$, DWs in the strong-penalization case propagate much faster than those in the weak-penalization case.

Acknowledgments.— A.G. thanks EPSRC for support under grant EP/K024116/1, J.M.R. thanks EPSRC for support under grant EP/K02390X/1, and V.S. thanks EPSRC for support under grants EP/I028714/1 and EP/K02390X/1.

-
- [1] S. S. P. Parkin, M. Hayashi and L. Thomas, *Science* **320**, 190 (2008).
[2] M. Hayashi, L. Thomas, R. Moriya, C. Rettner and S. S. P. Parkin, *Science* **320**, 209 (2008).
[3] L. Thomas, R. Moriya, C. Rettner, S. and S. P. Parkin, *Science* **330**, 1810 (2010).
[4] N. L. Schryer and L. R. Walker, *J. Appl. Phys.* **45**, 5406 (1974).
[5] J. Kirschner and R. Hertel, *Physica B: Cond. Mat.* **343**, 206 (2004).
[6] A. Mougin, M. Cormier, J. P. Adam, P. J. Metaxas, J. Ferré, *EPL* **78**, 57007 (2007).
[7] M.T. Bryan, T. Schrefl, D. Atkinson, D.A. Allwood, *J. Appl. Phys.* **103**, 073906 (2008).
[8] J. Yang, C. Nistor, G.S.D. Beach, and J.L. Erskine, *Phys. Rev. B* **77**, 014413 (2008).
[9] X.R. Wang, P. Yan, J. Lu, *Europhys. Lett.* **86**, 67001 (2009).
[10] X.R. Wang, P. Yan, J. Lu, C. He, *Ann. Phys.* **324**, 1815–1820 (2009).
[11] J. Lu and X.R. Wang, *J. Appl. Phys.* **107**, 083915 (2010).
[12] Z. Z. Sun and J. Schliemann, *Phys. Rev. Lett.* **104**, 037206 (2010).
[13] A. Goussev, J. M. Robbins, V. Slastikov, *Phys. Rev. Lett.* **104**, 147202 (2010).
[14] A. Goussev, R.G. Lund, J. M. Robbins, V. Slastikov, C. Sonnenberg, *Phys. Rev. B* **88**, 024425 (2013).
[15] A. Goussev, R.G. Lund, J. M. Robbins, V. Slastikov, C. Sonnenberg, *Proc. Roy. Soc. A* **469**, 20130308 (2013).
[16] L. Berger, *J. Appl. Phys.* **49**, 2156 (1978).
[17] L. Berger, *J. Appl. Phys.* **54**, 1954 (1984).
[18] L. Berger, *Phys. Rev. B* **54**, 9353 (1996).
[19] J.C. Slonczewski, *J. Magn. Magn. Mater.* **159**, L1 (1996).
[20] A. Thiaville, Y. Nakatani, J. Miltat, Y. Suzuki, *EPL* **69**, 990 (2005).
[21] M. Yan, A. Kákay, S. Gliga, R. Hertel, *Phys. Rev. Lett.* **104**, 057201 (2010).
[22] O. A. Tretiakov and Ar. Abanov, *Phys. Rev. Lett.* **105**, 157201 (2010).
[23] O. A. Tretiakov, Y. Liu, and Ar. Abanov, *Phys. Rev. Lett.* **108**, 247201 (2012).
[24] M. Yan, C. Andreas, A. Kákay, F. García-Sánchez, R. Hertel, *Appl. Phys. Lett.* **99**, 122505 (2011).
[25] Y. Gou, A. Goussev, J. M. Robbins, V. Slastikov, *Phys. Rev. B* **84**, 104445 (2011).
[26] A. Aharoni, *Introduction to the Theory of Ferromagnetism*, 2nd ed. (Clarendon Press, Oxford, 2001).
[27] L. D. Landau and E. M. Lifshitz, *Phys. Zeitsch. Sowjetunion* **8**, 153 (1935).
[28] T. L. Gilbert, *Phys. Rev.* **100**, 1243 (1955); *IEEE Trans. Mag.* **40**, 3443 (2004).
[29] G. Carbou, *Math. Models. Meth. Appl. Sci.* **11**, 1529 (2001).
[30] R. V. Kohn and V. Slastikov, *Arch. Rat. Mech. Anal.* **178**, 227 (2005).
[31] R. V. Kohn and V. Slastikov, *Proc. R. Soc. A* **461**, 143 (2005).